Precision measurements of $\mathcal{B}[\psi(3686) \to \pi^+\pi^- J/\psi]$ and $\mathcal{B}[J/\psi \to l^+l^-]$

M. Ablikim,[1] M. N. Achasov,[7,*] O. Albayrak,[4] D. J. Ambrose,[40] F. F. An,[1] Q. An,[41] J. Z. Bai,[1] R. Baldini Ferroli,[18a] Y. Ban,[27] J. Becker,[3] J. V. Bennett,[17] M. Bertani,[18a] J. M. Bian,[39] E. Boger,[20,†] O. Bondarenko,[21] I. Boyko,[20] S. Braun,[36] R. A. Briere,[4] V. Bytev,[20] H. Cai,[45] X. Cai,[1] O. Cakir,[35a] A. Calcaterra,[18a] G. F. Cao,[1] S. A. Cetin,[35b] J. F. Chang,[1] G. Chelkov,[20,†] G. Chen,[1] H. S. Chen,[1] J. C. Chen,[1] M. L. Chen,[1] S. J. Chen,[25] X. R. Chen,[22] Y. B. Chen,[1] H. P. Cheng,[15] Y. P. Chu,[1] D. Cronin-Hennessy,[39] H. L. Dai,[1] J. P. Dai,[1] D. Dedovich,[20] Z. Y. Deng,[1] A. Denig,[19] I. Denysenko,[20] M. Destefanis,[44a,44c] W. M. Ding,[29] Y. Ding,[23] L. Y. Dong,[1] M. Y. Dong,[1] S. X. Du,[47] J. Fang,[1] S. S. Fang,[1] L. Fava,[44b,44c] C. Q. Feng,[41] P. Friedel,[3] C. D. Fu,[1] J. L. Fu,[25] O. Fuks,[20,†] Y. Gao,[34] C. Geng,[41] K. Goetzen,[8] W. X. Gong,[1] W. Gradl,[19] M. Greco,[44a,44c] M. H. Gu,[1] Y. T. Gu,[10] Y. H. Guan,[37] A. Q. Guo,[26] L. B. Guo,[24] T. Guo,[24] Y. P. Guo,[26] Y. L. Han,[1] F. A. Harris,[38] K. L. He,[1] M. He,[1] Z. Y. He,[26] T. Held,[3] Y. K. Heng,[1] Z. L. Hou,[1] C. Hu,[24] H. M. Hu,[1] J. F. Hu,[36] T. Hu,[1] G. M. Huang,[5] G. S. Huang,[41] J. S. Huang,[13] L. Huang,[1] X. T. Huang,[29] Y. Huang,[25] T. Hussain,[43] C. S. Ji,[41] Q. Ji,[1] Q. P. Ji,[26] X. B. Ji,[1] X. L. Ji,[1] L. L. Jiang,[1] X. S. Jiang,[1] J. B. Jiao,[29] Z. Jiao,[15] D. P. Jin,[1] S. Jin,[1] F. F. Jing,[34] N. Kalantar-Nayestanaki,[21] M. Kavatsyuk,[21] B. Kloss,[19] B. Kopf,[3] M. Kornicer,[38] W. Kuehn,[36] W. Lai,[1] J. S. Lange,[36] M. Lara,[17] P. Larin,[12] M. Leyhe,[3] C. H. Li,[1] Cheng Li,[41] Cui Li,[41] D. M. Li,[47] F. Li,[1] G. Li,[1] H. B. Li,[1] J. C. Li,[1] K. Li,[11] Lei Li,[1] Q. J. Li,[1] W. D. Li,[1] W. G. Li,[1] X. L. Li,[29] X. N. Li,[1] X. Q. Li,[26] X. R. Li,[28] Z. B. Li,[33] H. Liang,[41] Y. F. Liang,[31] Y. T. Liang,[36] G. R. Liao,[34] X. T. Liao,[1] D. X. Lin,[12] B. J. Liu,[1] C. L. Liu,[4] C. X. Liu,[1] F. H. Liu,[30] Fang Liu,[1] Feng Liu,[5] H. Liu,[1] H. B. Liu,[10] H. H. Liu,[14] H. M. Liu,[1] H. W. Liu,[1] J. P. Liu,[45] K. Liu,[34] K. Y. Liu,[23] P. L. Liu,[29] Q. Liu,[37] S. B. Liu,[41] X. Liu,[22] Y. B. Liu,[26] Z. A. Liu,[1] Zhiqiang Liu,[1] Zhiqing Liu,[1] H. Loehner,[21] X. C. Lou,[1,‡] G. R. Lu,[13] H. J. Lu,[15] J. G. Lu,[1] X. R. Lu,[37] Y. P. Lu,[1] C. L. Luo,[24] M. X. Luo,[46] T. Luo,[38] X. L. Luo,[1] M. Lv,[1] F. C. Ma,[23] H. L. Ma,[1] Q. M. Ma,[1] S. Ma,[1] T. Ma,[1] X. Y. Ma,[1] F. E. Maas,[12] M. Maggiora,[44a,44c] Q. A. Malik,[43] Y. J. Mao,[27] Z. P. Mao,[1] J. G. Messchendorp,[21] J. Min,[1] T. J. Min,[1] R. E. Mitchell,[17] X. H. Mo,[1] H. Moeini,[21] C. Morales Morales,[12] K. Moriya,[17] N. Yu. Muchnoi,[7,*] H. Muramatsu,[40] Y. Nefedov,[20] I. B. Nikolaev,[7,*] Z. Ning,[1] S. L. Olsen,[28] Q. Ouyang,[1] S. Pacetti,[18b] J. W. Park,[38] M. Pelizaeus,[3] H. P. Peng,[41] K. Peters,[8] J. L. Ping,[24] R. G. Ping,[1] R. Poling,[39] E. Prencipe,[19] M. Qi,[25] S. Qian,[1] C. F. Qiao,[37] L. Q. Qin,[29] X. S. Qin,[1] Y. Qin,[27] Z. H. Qin,[1] J. F. Qiu,[1] K. H. Rashid,[43] C. F. Redmer,[19] G. Rong,[1] X. D. Ruan,[10] A. Sarantsev,[20,§] M. Shao,[41] C. P. Shen,[2] X. Y. Shen,[1] H. Y. Sheng,[1] M. R. Shepherd,[17] W. M. Song,[1] X. Y. Song,[1] S. Spataro,[44a,44c] B. Spruck,[36] D. H. Sun,[1] G. X. Sun,[1] J. F. Sun,[13] S. S. Sun,[1] Y. J. Sun,[41] Y. Z. Sun,[1] Z. J. Sun,[1] Z. T. Sun,[41] C. J. Tang,[31] X. Tang,[1] I. Tapan,[35c] E. H. Thorndike,[40] D. Toth,[39] M. Ullrich,[36] I. Uman,[35b] G. S. Varner,[38] B. Wang,[1] D. Wang,[27] D. Y. Wang,[27] K. Wang,[1] L. L. Wang,[1] L. S. Wang,[1] M. Wang,[29] P. Wang,[1] P. L. Wang,[1] Q. J. Wang,[1] S. G. Wang,[27] X. F. Wang,[34] X. L. Wang,[41] Y. D. Wang,[18a] Y. F. Wang,[1] Y. Q. Wang,[19] Z. Wang,[1] Z. G. Wang,[1] Z. Y. Wang,[1] D. H. Wei,[9] J. B. Wei,[27] P. Weidenkaff,[19] Q. G. Wen,[41] S. P. Wen,[1] M. Werner,[36] U. Wiedner,[3] L. H. Wu,[1] N. Wu,[1] S. X. Wu,[41] W. Wu,[26] Z. Wu,[1] L. G. Xia,[34] Y. X. Xia,[16] Z. J. Xiao,[24] Y. G. Xie,[1] Q. L. Xiu,[1] G. F. Xu,[1] Q. J. Xu,[11] Q. N. Xu,[37] X. P. Xu,[32] Z. R. Xu,[41] Z. Xue,[1] L. Yan,[41] W. B. Yan,[41] Y. H. Yan,[16] H. X. Yang,[1] Y. Yang,[5] Y. X. Yang,[9] H. Ye,[1] M. Ye,[1] M. H. Ye,[6] B. X. Yu,[1] C. X. Yu,[26] H. W. Yu,[27] J. S. Yu,[22] S. P. Yu,[29] C. Z. Yuan,[1] Y. Yuan,[1] A. A. Zafar,[43] A. Zallo,[18a] S. L. Zang,[25] Y. Zeng,[16] B. X. Zhang,[1] B. Y. Zhang,[1] C. Zhang,[25] C. C. Zhang,[1] D. H. Zhang,[1] H. H. Zhang,[33] H. Y. Zhang,[1] J. Q. Zhang,[1] J. W. Zhang,[1] J. Y. Zhang,[1] J. Z. Zhang,[1] LiLi Zhang,[16] R. Zhang,[37] S. H. Zhang,[1] X. J. Zhang,[1] X. Y. Zhang,[29] Y. Zhang,[1] Y. H. Zhang,[1] Z. P. Zhang,[41] Z. Y. Zhang,[45] Zhenghao Zhang,[5] G. Zhao,[1] H. S. Zhao,[1] J. W. Zhao,[1] Lei Zhao,[41] Ling Zhao,[1] M. G. Zhao,[26] Q. Zhao,[1] S. J. Zhao,[47] T. C. Zhao,[1] X. H. Zhao,[25] Y. B. Zhao,[1] Z. G. Zhao,[41] A. Zhemchugov,[20,†] B. Zheng,[42] J. P. Zheng,[1] Y. H. Zheng,[37] B. Zhong,[24] L. Zhou,[1] X. Zhou,[45] X. K. Zhou,[37] X. R. Zhou,[41] C. Zhu,[1] K. Zhu,[1] K. J. Zhu,[1] S. H. Zhu,[1] X. L. Zhu,[34] Y. C. Zhu,[41] Y. S. Zhu,[1] Z. A. Zhu,[1] J. Zhuang,[1] B. S. Zou,[1] and J. H. Zou[1]

(BESIII Collaboration)

[1]*Institute of High Energy Physics, Beijing 100049, People's Republic of China*
[2]*Beihang University, Beijing 100191, People's Republic of China*
[3]*Bochum Ruhr-University, D-44780 Bochum, Germany*
[4]*Carnegie Mellon University, Pittsburgh, Pennsylvania 15213, USA*
[5]*Central China Normal University, Wuhan 430079, People's Republic of China*
[6]*China Center of Advanced Science and Technology, Beijing 100190, People's Republic of China*
[7]*G.I. Budker Institute of Nuclear Physics SB RAS (BINP), Novosibirsk 630090, Russia*
[8]*GSI Helmholtzcentre for Heavy Ion Research GmbH, D-64291 Darmstadt, Germany*
[9]*Guangxi Normal University, Guilin 541004, People's Republic of China*

[10]*GuangXi University, Nanning 530004, People's Republic of China*
[11]*Hangzhou Normal University, Hangzhou 310036, People's Republic of China*
[12]*Helmholtz Institute Mainz, Johann-Joachim-Becher-Weg 45, D-55099 Mainz, Germany*
[13]*Henan Normal University, Xinxiang 453007, People's Republic of China*
[14]*Henan University of Science and Technology, Luoyang 471003, People's Republic of China*
[15]*Huangshan College, Huangshan 245000, People's Republic of China*
[16]*Hunan University, Changsha 410082, People's Republic of China*
[17]*Indiana University, Bloomington, Indiana 47405, USA*
[18a]*INFN Laboratori Nazionali di Frascati, I-00044 Frascati, Italy*
[18b]*INFN and University of Perugia, I-06100 Perugia, Italy*
[19]*Johannes Gutenberg University of Mainz, Johann-Joachim-Becher-Weg 45, D-55099 Mainz, Germany*
[20]*Joint Institute for Nuclear Research, 141980 Dubna, Moscow region, Russia*
[21]*KVI, University of Groningen, NL-9747 AA Groningen, The Netherlands*
[22]*Lanzhou University, Lanzhou 730000, People's Republic of China*
[23]*Liaoning University, Shenyang 110036, People's Republic of China*
[24]*Nanjing Normal University, Nanjing 210023, People's Republic of China*
[25]*Nanjing University, Nanjing 210093, People's Republic of China*
[26]*Nankai university, Tianjin 300071, People's Republic of China*
[27]*Peking University, Beijing 100871, People's Republic of China*
[28]*Seoul National University, Seoul, 151-747 Korea*
[29]*Shandong University, Jinan 250100, People's Republic of China*
[30]*Shanxi University, Taiyuan 030006, People's Republic of China*
[31]*Sichuan University, Chengdu 610064, People's Republic of China*
[32]*Soochow University, Suzhou 215006, People's Republic of China*
[33]*Sun Yat-Sen University, Guangzhou 510275, People's Republic of China*
[34]*Tsinghua University, Beijing 100084, People's Republic of China*
[35a]*Ankara University, Dogol Caddesi, 06100 Tandogan, Ankara, Turkey*
[35b]*Dogus University, 34722 Istanbul, Turkey*
[35c]*Uludag University, 16059 Bursa, Turkey*
[36]*Universitaet Giessen, D-35392 Giessen, Germany*
[37]*University of Chinese Academy of Sciences, Beijing 100049, People's Republic of China*
[38]*University of Hawaii, Honolulu, Hawaii 96822, USA*
[39]*University of Minnesota, Minneapolis, Minnesota 55455, USA*
[40]*University of Rochester, Rochester, New York 14627, USA*
[41]*University of Science and Technology of China, Hefei 230026, People's Republic of China*
[42]*University of South China, Hengyang 421001, People's Republic of China*
[43]*University of the Punjab, Lahore-54590, Pakistan*
[44a]*University of Turin, I-10125 Turin, Italy*
[44b]*University of Eastern Piedmont, I-15121 Alessandria, Italy*
[44c]*INFN, I-10125 Turin, Italy*
[45]*Wuhan University, Wuhan 430072, People's Republic of China*
[46]*Zhejiang University, Hangzhou 310027, People's Republic of China*
[47]*Zhengzhou University, Zhengzhou 450001, People's Republic of China*

(Received 4 July 2013; published 12 August 2013)

Based on $(106.41 \pm 0.86) \times 10^6$ $\psi(3686)$ events collected with the BESIII detector at the BEPCII collider, the branching fractions of $\psi(3686) \to \pi^+\pi^- J/\psi$, $J/\psi \to e^+e^-$, and $J/\psi \to \mu^+\mu^-$ are measured. We obtain $\mathcal{B}[\psi(3686) \to \pi^+\pi^- J/\psi] = (34.98 \pm 0.02 \pm 0.45)\%$, $\mathcal{B}[J/\psi \to e^+e^-] = (5.983 \pm 0.007 \pm 0.037)\%$, and $\mathcal{B}[J/\psi \to \mu^+\mu^-] = (5.973 \pm 0.007 \pm 0.038)\%$. The measurement of $\mathcal{B}[\psi(3686) \to \pi^+\pi^- J/\psi]$ confirms the CLEO-c measurement, and is apparently larger than the others. The measured J/ψ leptonic decay branching fractions agree with previous experiments within one standard deviation. These results lead to $\mathcal{B}[J/\psi \to l^+l^-] = (5.978 \pm 0.005 \pm 0.040)\%$ by averaging

[*]Also at the Novosibirsk State University, Novosibirsk, 630090, Russia.
[†]Also at the Moscow Institute of Physics and Technology, Moscow 141700, Russia.
[‡]Also at University of Texas at Dallas, Richardson, Texas 75083, USA.
[§]Also at the PNPI, Gatchina 188300, Russia.
[‖]Also with Università della Basilicata, Potenza, Italy.
[¶]Also with Università di Sassari, Sassari, Italy.

over the e^+e^- and $\mu^+\mu^-$ channels and a ratio of $\mathcal{B}[J/\psi \to e^+e^-]/\mathcal{B}[J/\psi \to \mu^+\mu^-] = 1.0017 \pm 0.0017 \pm 0.0033$, which tests e-μ universality at the four tenths of a percent level. All the measurements presented in this paper are the most precise in the world to date.

DOI: 10.1103/PhysRevD.88.032007 PACS numbers: 13.25.Gv, 13.20.Gd, 14.40.Pq

I. INTRODUCTION

Since the discovery almost four decades ago of the first charmonium state, the J/ψ [1], the states that have been studied the most among the various conventional charmonium states found have been the J/ψ and $\psi(3686)$. However, the largest branching fraction in $\psi(3686)$ decays, $\mathcal{B}[\psi(3686) \to \pi^+\pi^- J/\psi](\mathcal{B}_{\pi\pi J/\psi})$, still remains interesting both experimentally and theoretically. On the experimental side, the mass recoiling against the dipion system ($M^{\rm rec}_{\pi^+\pi^-}$) of this common decay mode can be used to identify J/ψ decays. This makes $\mathcal{B}_{\pi\pi J/\psi}$ crucial for the relevant measurements in charmonium decays and in searches for new particles, such as invisible particles in J/ψ decays, as well as the measurements of charmonium production rates in higher-energy collisions. Because of its large size, the branching fraction, $\mathcal{B}_{\pi\pi J/\psi}$, also imposes a limit on the rest of the decay channels of $\psi(3686)$. On the theoretical side, the transition $\psi(3686) \to \pi^+\pi^- J/\psi$ relates to the interaction between heavy quarks and gluons as well as hadronization, providing an excellent testing ground for some theoretical predictions, such as the QCD multipole expansion [2] and chiral symmetry [3].

The measured value of $\mathcal{B}_{\pi\pi J/\psi}$, however, has changed dramatically in the last decades [4–8]. For example, the most recent result from CLEO-c, $\mathcal{B}_{\pi\pi J/\psi} = (35.04 \pm 0.8)\%$ [5], is apparently larger than the former most precise result of $(32.3 \pm 1.4)\%$ from BESII [8]. The situation, thus, demands additional, high-precision measurements of $\mathcal{B}_{\pi\pi J/\psi}$. The data sample of $\psi(3686)$ collected with the BESIII detector, which is the world's largest such sample, makes it possible to remeasure $\mathcal{B}_{\pi\pi J/\psi}$ and clarify the discrepancy.

Similar to the transition $\psi(3686) \to \pi^+\pi^- J/\psi$, $J/\psi \to e^+e^-$ and $\mu^+\mu^-$ are often used to identify the J/ψ experimentally for they are the two largest and cleanest decay modes of J/ψ. The branching fractions for the leptonic decays $J/\psi \to e^+e^-(\mathcal{B}_{ee})$ and $J/\psi \to \mu^+\mu^-(\mathcal{B}_{\mu\mu})$ are fundamental parameters of the J/ψ resonance, and hence of general interest. The process of a vector charmonium decaying into a lepton pair is thought to occur through the annihilation of the $c\bar{c}$ pair into a virtual photon, and thereby is related to the $c\bar{c}$ wave-function overlap at the origin, which plays a direct role in potential models [9]. Furthermore, the ratio $\mathcal{B}_{ee}/\mathcal{B}_{\mu\mu}$ provides a test of lepton universality. The standard model predicts exact lepton universality for ee and $\mu\mu$, and any deviation from unity will indicate possible new physics effects or new decay mechanisms for J/ψ to l^+l^-, where l may be either e or μ. Also, as the branching fraction of $J/\psi \to l^+l^-$ ($\mathcal{B}_{ll}$) is important in the determination of the J/ψ leptonic and total widths, (Γ_{ee} and $\Gamma_{\rm tot}$) [10], its precision is important for their uncertainties.

$\mathcal{B}_{ee}$ and $\mathcal{B}_{\mu\mu}$ have been measured to be approximately equal, as expected from lepton universality combined with a negligible phase-space correction. A relative precision of 1% on both $\mathcal{B}_{ee}$ and $\mathcal{B}_{\mu\mu}$ has been achieved through an average [11] over measurements, which are dominated by the results from CLEO-c [12] and BESI [13].

This paper describes the measurement of the branching fraction $\mathcal{B}_{\pi\pi J/\psi}$, as well as $\mathcal{B}_{ll}$ via the decay $\psi(3686) \to \pi^+\pi^- J/\psi$. Measuring $\mathcal{B}_{ll}$ via $\psi(3686) \to \pi^+\pi^- J/\psi$ has the advantage that there is no interference with Bhabha or dimuon production, which would need to be considered in measurements via direct J/ψ production and decay in an electron-positron collider.

Our overall analysis procedure is as follows. The observed number of events, $N_{\pi\pi J/\psi}$ and N_{ll} (ll represents $\pi^+\pi^- l^+l^-$ final states), are extracted by fitting to data distributions or counting the signal candidate events directly. The corresponding acceptances, $\epsilon_{\pi\pi J/\psi}$ and ϵ_{ll}, are calculated based on Monte Carlo (MC) samples. Then $\mathcal{B}_{\pi\pi\psi}$ is calculated with the equation

$$\mathcal{B}_{\pi\pi J/\psi} = \frac{N_{\pi\pi J/\psi}}{\epsilon_{\pi\pi J/\psi} \times N_{\rm tot}}, \tag{1}$$

where $N_{\rm tot}$ is the number of $\psi(3686)$ events. $\mathcal{B}_{ll}$ is calculated with

$$\begin{aligned}\mathcal{B}_{ll} &= \frac{\mathcal{B}_{\pi\pi J/\psi} \times \mathcal{B}_{ll}}{\mathcal{B}_{\pi\pi J/\psi}} \\ &= \frac{N_{ll}/(\epsilon_{ll} \times N_{\rm tot})}{N_{\pi\pi J/\psi}/(\epsilon_{\pi\pi J/\psi} \times N_{\rm tot})} \\ &= \frac{N_{ll}/\epsilon_{ll}}{N_{\pi\pi J/\psi}/\epsilon_{\pi\pi J/\psi}}.\end{aligned} \tag{2}$$

Here it should be noted that Eq. (2) is independent of the number of $\psi(3686)$ events, which is one of the major sources of systematic uncertainties in the determination of $\mathcal{B}_{\pi\pi J/\psi}$.

II. BEPCII AND BESIII

BESIII/BEPCII, described in detail in Ref. [14], is a major upgrade of the BESII detector and the BEPC accelerator [15] for studies of hadron spectroscopy and τ-charm physics [16]. The design peak luminosity of the

double-ring e^+e^- collider, BEPCII, is 10^{33} cm^{-2} s^{-1} at a beam current of 0.93 A.

The BESIII detector, with a geometrical acceptance of 93% of 4π, consists of the following main components. 1) A main drift chamber (MDC) equipped with 6796 signal wires and 21 884 field wires arranged in a small-cell configuration with 43 layers working in a gas mixture of He (40%) and C_3H_8 (60%). The single wire resolution on average is 135 μm, and the momentum resolution for charged particles in a 1 T magnetic field is 0.5% at 1 GeV/c. 2) An electromagnetic calorimeter (EMC) made of 6240 CsI (Tl) crystals arranged in a cylindrical shape plus two end-caps. The energy resolution is 2.5% in the barrel and 5% in the end-caps at 1.0 GeV; the position resolution is 6 mm in the barrel and 9 mm in the end-caps at 1.0 GeV. 3) A time-of-flight system (TOF) for particle identification with a cylindrically shaped barrel portion, made with two layers with 176 pieces of 5-cm-thick, 2.4-m-long plastic scintillators in each layer, and end-caps each with 96 fan-shaped, 5-cm-thick plastic scintillators. The time resolution is 80 ps in the barrel, and 110 ps in the end-caps, corresponding to a K/π separation at the 2σ level up to about 1.0 GeV/c. 4) A muon chamber system (MUC) made of 1000 m^2 of resistive plate chambers (RPC) arranged in nine layers in the barrel and eight layers in the end-caps. The position resolution is about 2 cm.

III. EVENT SELECTION

The data sample used for this analysis consists of $(106.41 \pm 0.86) \times 10^6$ $\psi(3686)$ decays produced at the resonance peak [17] and an additional 44 pb^{-1} of data collected at $\sqrt{s} = 3.65$ GeV to determine the nonresonant background contributions. A MC sample of 106×10^6 $\psi(3686)$ inclusive decay events is used to obtain the detection efficiencies as well as to estimate the backgrounds. This sample is generated with KKMC [18] and EVTGEN [19] for decays with known branching fractions [20], or by LUNDCHARM [21] for unmeasured decays. In this sample, the signal process of $\psi(3686) \to \pi^+\pi^- J/\psi$ is generated according to the formulas and measured results in Ref. [22], which takes the small D-wave contribution into account; the $J/\psi \to l^+l^-$ processes are generated with an angular distribution of $(1 + \cos^2\theta_l)$, where θ_l is the lepton angle relative to the beam line in the J/ψ rest frame, and PHOTOS [23] is used for the final-state radiation. These MC events are then processed with the detector simulation package based on GEANT4 [24].

In order to suppress tracks due to cosmic rays and beam-associated events, charged tracks are required to pass within ± 10 cm of the run-by-run determined interaction point along the beam direction and within 1 cm of the beam line in the plane perpendicular to the beam. To guarantee good agreement between data and MC simulation, all the charged tracks must lie in the barrel region, i.e., $|\cos\theta| < 0.8$, where θ is the polar angle with respect to the positron beam direction.

To identify $\pi^+\pi^- J/\psi$ candidates, $M^{\rm rec}_{\pi^+\pi^-}$ is determined for all pairs of charged tracks of opposite charge with momentum less than 450 MeV/c, which are assumed to be pions, and all the combinations with $M^{\rm rec}_{\pi^+\pi^-}$ near the J/ψ peak are kept ([3.04, 3.16] GeV/c^2). The $(n)\gamma J/\psi$ backgrounds with an electron-positron pair converted from a photon are removed by requiring the cosine of the angle between the two charged tracks in the laboratory frame be less than 0.95. $N_{\pi\pi J/\psi}$ is determined from a fit to the distribution of $M^{\rm rec}_{\pi^+\pi^-}$. The left plot in Fig. 1 shows the distribution of $M^{\rm rec}_{\pi^+\pi^-}$ for data, non-$\pi^+\pi^- J/\psi$ decays, the scaled continuum events, and the sum of the signal from MC simulation and all backgrounds. Note that the mass resolutions of data (black dots) and MC simulation (red histogram) are different, which is considered in the following sections.

For the selection of $\pi^+\pi^- l^+l^-$ candidates, the pion pair is identified in the same way as for $\pi^+\pi^- J/\psi$. When multiple entries occur, the one with the minimum $|M^{\rm rec}_{\pi^+\pi^-} - m_{J/\psi}|$ is kept, where $m_{J/\psi}$ is the nominal J/ψ mass [11]. The fastest positive and negative tracks are taken as the lepton candidates. The lepton species are identified with their E/p ratios, where E is the measured energy deposition in the EMC of each track and p is its measured momentum. The events with both $[E/p]^+ < 0.26$ and $[E/p]^- < 0.26$ are taken as $\mu^+\mu^-$ events, and those with $[E/p]^+ > 0.80$, $[E/p]^- > 0.80$, or

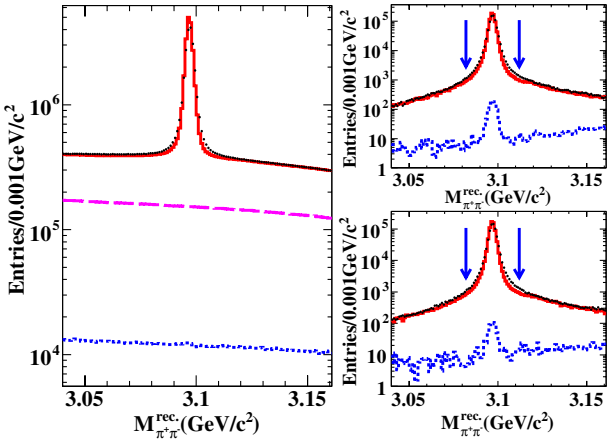

FIG. 1 (color online). (left) Distributions of $M^{\rm rec}_{\pi^+\pi^-}$, where candidate events are represented by black dots, the non-$\pi^+\pi^- J/\psi$ decays of $\psi(3686)$ background by the purple long dashed line, the scaled continuum by the blue dashed dotted line, and the $\psi(3686)$ inclusive MC plus the scaled continuum and non-$\pi^+\pi^- J/\psi$ background by the red histogram. Distributions of $M^{\rm rec}_{\pi^+\pi^-}$ $J/\psi \to e^+e^-$ (top right) and $J/\psi \to \mu^+\mu^-$ (bottom right) candidate events are shown, where only total backgrounds are shown with blue dash-dotted lines. The arrows indicate the mass windows to count the number of signal candidates.

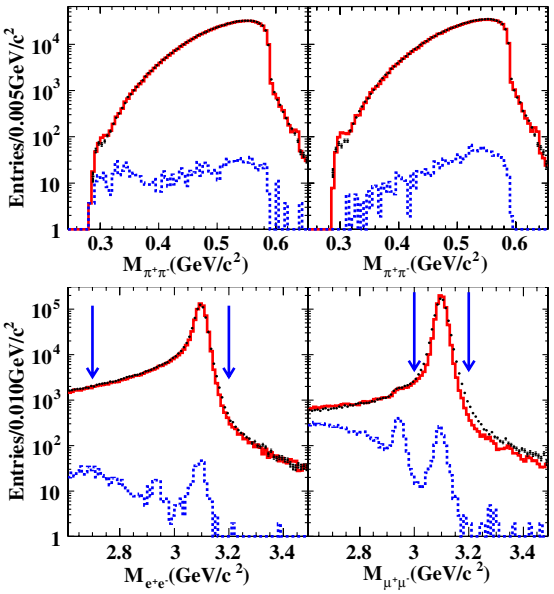

FIG. 2 (color online). Distributions of $\psi(3686) \to \pi^+\pi^- J/\psi$, $J/\psi \to e^+e^-$ (left) and $J/\psi \to \mu^+\mu^-$ (right) candidate events in the $\psi(3686)$ data (black dots with error bars), MC simulation of signal plus background (red solid histogram), and backgrounds (blue dashed dotted line). The top panel shows distributions of the dipion invariant mass, and the bottom panel shows the dilepton invariant mass. The arrows shown in each plot indicate nominal selection criteria, which are applied for the other plots in the figure.

$\sqrt{([E/p]^+ - 1)^2 + ([E/p]^- - 1)^2} < 0.4$ are taken as e^+e^- events. The backgrounds, such as $J/\psi \to \pi^+\pi^-\pi^0$, are removed by requiring that the cosine of the angle between two lepton candidates in the laboratory frame be less than -0.95. The invariant mass of the lepton pair must be consistent with that of a J/ψ, i.e., $M_{e^+e^-} \in [2.7, 3.2]$ GeV/c^2 or $M_{\mu^+\mu^-} \in [3.0, 3.2]$ GeV/c^2, where different mass windows are used since the e^+e^- final state has more final state radiation than $\mu^+\mu^-$ does. Figure 2 shows the invariant masses of the dipion pair (top) and the dilepton pairs (bottom) for $\pi^+\pi^- e^+e^-$ (left) and $\pi^+\pi^-\mu^+\mu^-$ (right) final states. To extract N_{ll}, we count the number of events directly in a narrower mass window of $M^{\rm rec}_{\pi\pi}$. Figure 1 shows the distributions of the invariant mass recoiling against the dipion for the e^+e^- (top right) and $\mu^+\mu^-$ (bottom right) channels for the $\pi^+\pi^- l^+ l^-$ candidates.

IV. BACKGROUND STUDY

For the $\pi^+\pi^- J/\psi$ final state, the backgrounds are studied with the $\psi(3686)$ inclusive MC and the continuum data sample. The backgrounds can be classified into three categories: 1) the non-$\pi^+\pi^- J/\psi$ decays of $\psi(3686)$, such as $\psi(3686) \to$ light hadrons or $\psi(3686) \to \eta J/\psi$; 2) the $\psi(3686) \to \pi^+\pi^- J/\psi$ decays, but one or both soft pions are from J/ψ decays; and 3) other backgrounds, including the continuum process in e^+e^- annihilation, and beam-related and cosmic-ray backgrounds. As shown in the left plot of Fig. 1, the backgrounds from the non-$\pi^+\pi^- J/\psi$ and non-$\psi(3686)$ events are smooth and produce no peak at the J/ψ mass. The second kind of background is studied with a toy MC simulation in which the contributions with one or two charged tracks from J/ψ decays are studied. The background shape is also found to be smooth with no peak at J/ψ mass.

After all the requirements described above, the $\pi^+\pi^- l^+ l^-$ event samples are rather clean. In the window of the invariant mass recoiling against the dipion $[m_{J/\psi} - 15, m_{J/\psi} + 15]$ MeV/c^2, for the $\pi^+\pi^- e^+e^-$ final state, the background level is estimated to be less than 0.10%. The largest background is $\psi(3686) \to \eta J/\psi$, $\eta \to \gamma\pi^+\pi^-$, $J/\psi \to e^+e^-$ ($\sim$0.04%), and the second largest background is $\psi(3686) \to \pi^+\pi^- J/\psi$, $J/\psi \to \pi^+\pi^-\pi^0$ ($\sim$0.03%). For the $\pi^+\pi^-\mu^+\mu^-$ final state, the total background level is found to be 0.15%. The largest background is from $\psi(3686) \to \pi^+\pi^- J/\psi$, $J/\psi \to \pi^+\pi^-$ ($\sim$0.09%), and the second largest background is $\psi(3686) \to \eta J/\psi$, $\eta \to \gamma\pi^+\pi^-$, $J/\psi \to \mu^+\mu^-$ ($\sim$0.02%). Since the dominant backgrounds are exclusively simulated and subtracted from the signal region according to the known branching fractions and the scaled continuum data is subtracted, the remaining background is only 0.03 (0.04)% for the $e^+e^-(\mu^+\mu^-)$ channel.

V. DATA ANALYSIS

Since the dipion emission occurs independently of the subsequent J/ψ decay, the dipion recoil mass shape can be taken from any cleanly determined J/ψ decay. We use $J/\psi \to e^+e^-$, which is almost background free and has less background than $J/\psi \to \mu^+\mu^-$, for the signal shape of the dipion recoil mass distribution, and use a second-order polynomial to model the background shape. Increasing the order of the polynomial does not substantially improve the fit. However, a study shows that the resolution of the $\pi^+\pi^-$ recoil mass depends on the charged track multiplicity of J/ψ decays. As a result, the mass resolution from leptonic exclusive decays of J/ψ is slightly better than that of J/ψ inclusive decays, and the difference produces a bad fit quality (χ^2/d.o.f.) $\sim$ 50, where d.o.f. is the number of degrees of freedom). To improve the fit quality, the signal shapes are smeared by convoluting them with two Gaussian functions, whose parameters are determined by directly fitting to data. While this procedure obviously improves the quality (χ^2/d.o.f. $\sim$ 4), it changes the resultant $\mathcal{B}_{\pi\pi J/\psi}$ by only 0.37%, which is taken as one of the sources of systematic uncertainty. Figure 3 shows the fit to the dipion recoil mass spectrum for $\psi(3686) \to \pi^+\pi^- J/\psi$, $J/\psi \to$ anything.

For the $\pi^+\pi^- l^+ l^-$ final states, the number of signal candidates in the distribution of $M^{\rm rec}_{\pi^+\pi^-}$ are counted directly, since they are almost background free. However,

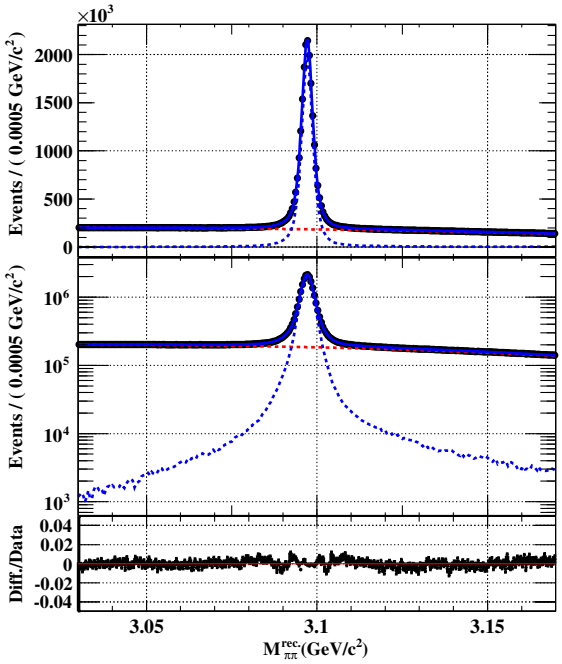

FIG. 3 (color online). The dipion recoil mass spectrum for $\psi(3686) \to \pi^+\pi^- J/\psi$, $J/\psi \to$ anything. Top: Data points (black) overlaid with the fit result (solid blue curve) obtained using the signal shape from $\psi(3686) \to \pi^+\pi^- J/\psi$, $J/\psi \to e^+e^-$ (blue dashed curve) and a second-order polynomial background shape (red dashed curve). Middle: The same plot as the top but with a log scale. Bottom: The fractional difference between the fit and the data.

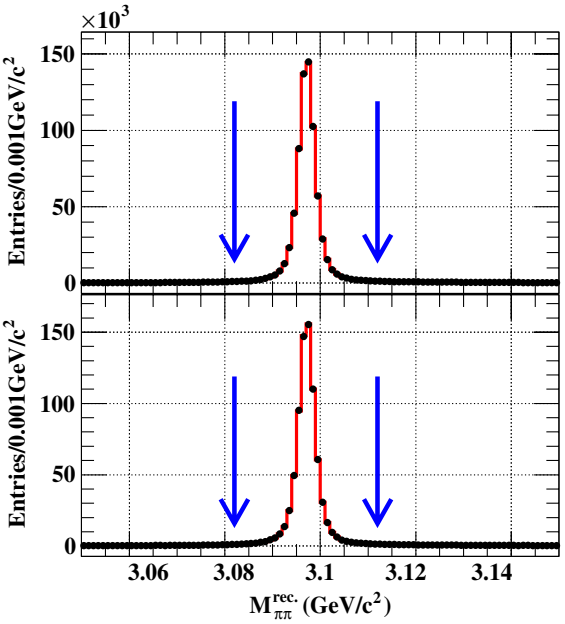

FIG. 4 (color online). The dipion recoil mass spectrum for $\psi(3686) \to \pi^+\pi^- J/\psi$, $J/\psi \to l^+l^-$, with the data points (black dots) overlaid with the smeared MC simulation (solid red histogram) according to the signal shape of data. The regions between the arrows are used to count the number of candidates. Top: $J/\psi \to e^+e^-$. Bottom: $J/\psi \to \mu^+\mu^-$.

TABLE I. Summary of MC input/output check results of the three processes ($\mathcal{B}$ is in percent).

Modes	$\mathcal{B}_{\rm in}$	$N_{\rm obs}(10^3)$	$\mathcal{B}$
$\pi^+\pi^- J/\psi$	32.6	18783.4 ± 5.1	32.64 ± 0.03
$\pi^+\pi^- e^+e^-$	5.93	660.6 ± 0.8	5.912 ± 0.024
$\pi^+\pi^- \mu^+\mu^-$	5.94	707.5 ± 0.8	5.930 ± 0.024

TABLE II. Summary of $\psi(3686) \to \pi^+\pi^- J/\psi$ and $J/\psi \to l^+l^-$ results, showing numbers of the three decays ($N_{\pi\pi J/\psi}$, N_{ee}, and $N_{\mu\mu}$), the efficiencies for observing those decays ($\epsilon_{\pi\pi J/\psi}$, ϵ_{ee} and $\epsilon_{\mu\mu}$), and the calculated branching fractions of the three channels, along with the statistical uncertainties on all quantities.

	$\pi^+\pi^- J/\psi$	$\pi^+\pi^- e^+e^-$	$\pi^+\pi^- \mu^+\mu^-$
$N(10^3)$	20235 ± 6	718.8 ± 0.9	771.1 ± 0.9
$\epsilon(\%)$	54.37 ± 0.02	32.19 ± 0.04	34.54 ± 0.04
$\mathcal{B}(\%)$	34.98 ± 0.02	5.983 ± 0.007	5.973 ± 0.007

as shown in the right column of Fig. 1, the resolutions of data (black dots) and MC simulation (red histogram) are different. Thus, the MC distributions are smeared according to data in determining their reconstruction efficiencies. A mass window of $[m_{J/\psi} - 15, m_{J/\psi} + 15]$ MeV/c^2 ($\sim 5\sigma$) is used in counting the signal candidates. Figure 4 shows the comparison between data and the smeared MC simulation, in which the data points, as well as the regions, are the same as those in the right panel of Fig. 1.

To validate the analysis method, MC input/output checks are performed based on the 106×10^6 $\psi(3686)$ inclusive MC sample, which has input values $\mathcal{B}_{\pi\pi J/\psi}$, $\mathcal{B}_{ee}$, and $\mathcal{B}_{\mu\mu}$ of 32.6%, 5.93%, and 5.94%, respectively. Since this sample cannot be used at the same time to determine the efficiencies, an alternative 10^7 $\psi(3686)$ inclusive MC sample with the same configuration described in Sec. III is used for their determination. In order to make these two samples look more like real data, we also add in the scaled continuum data. As shown in Table I, all the extracted branching fractions are consistent with the input branching fractions within their uncertainties.

Table II summarizes the resultant signal yields, efficiencies, and branching fractions based on data, along with their statistical uncertainties.

VI. STUDY OF SYSTEMATIC UNCERTAINTIES

We consider systematic uncertainties from many different sources. The uncertainty of the number of $\psi(3686)$ decays, 0.81% [17], which is measured by counting the hadronic events from $\psi(3686)$ decay directly, is the dominant uncertainty of $\mathcal{B}_{\pi\pi J/\psi}$, while $\mathcal{B}_{ee}$ and $\mathcal{B}_{\mu\mu}$ are independent of it. The difference of tracking efficiency between data and MC simulation is measured from a comparison of

yields of partially and fully reconstructed $\psi(3686) \to \pi^+\pi^- J/\psi$ and $J/\psi \to l^+l^-$ decays in real and simulated data. The differences depending on the polar angle and the transverse momentum of the track are used to reweight the MC samples. The uncertainty of the reweighting factor is estimated to be 0.1% per lepton and 0.4% per pion. The systematic effects related to the soft pion tracking cancel in the calculation of $\mathcal{B}_{ee}$ and $\mathcal{B}_{\mu\mu}$. The tracking uncertainties of π^+ and π^- or l^+ and l^- are considered as fully correlated and are added linearly.

In the inclusive analysis, even though we only reconstruct two soft charged pions, the reconstruction efficiency depends on the track multiplicity of the subsequent J/ψ decays. However, since the sum of known exclusive J/ψ partial widths is small compared to the total width, a MC sample must be used to represent all J/ψ decays and to obtain $\epsilon_{\pi\pi J/\psi}$. The global efficiency found is about 54% but varies by about 15% (relative) from low to high charged-track multiplicities of J/ψ decays, similar to that reported in BESI [13], but the variation is much larger than that in CLEO-c [12]. We attribute the difference to the finer segmentation in the CLEO-c tracking system, which was designed for physics at higher energy [25] relative to that of BESI [26] and BESIII [14], as well as the consequent robustness of track reconstruction in the presence of many charged particles.

To study the dependence of the detection efficiency $\epsilon_{\pi\pi J/\psi}$ on the generated charged track multiplicity distribution for J/ψ decays in $\pi^+\pi^- J/\psi$ events, we first use the inclusive MC sample to determine the detection efficiency (ϵ_k) as a function of generated track multiplicity (k), as shown in Table III, and then determine $\epsilon_{\pi\pi J/\psi}$ considering alternative generated multiplicity distributions. Two methods are used to determine the fraction w_k of each multiplicity from data directly and $\epsilon_{\pi\pi J/\psi}$. The first is the method used in Ref. [13], which fits the observed multiplicities in data using the efficiency matrix, ϵ_{ij}, which describes the efficiency of a MC event generated with j charged tracks to be reconstructed with i charged tracks, to determine the true generated charged track multiplicity distribution. The second method fits the observed multiplicity distribution with exclusive MC-based templates, as in Ref. [12]. Figure 5 shows the multiplicity distribution fitted by the generated multiplicity distribution of the inclusive MC. Table III summarizes the multiplicity distribution obtained from the $\psi(3686)$ inclusive MC and the two methods mentioned above, as well as the overall $\epsilon_{\pi\pi J/\psi}$ for each case. Consistent results are obtained, which indicates that $\epsilon_{\pi\pi J/\psi}$ is not very sensitive to the generated multiplicity distribution of J/ψ decays. We assign the largest difference as the systematic uncertainty due to our imperfect simulation of the charged track multiplicity, $N_{\rm trk}^{J/\psi}$, in J/ψ decays.

TABLE III. The fractions of each charged track multiplicity of J/ψ decays from the $\psi(3686)$ inclusive MC (column 2), from the method of Ref. [13] (column 3), and that of Ref. [12] (column 4). The MC efficiency for k-charged tracks is shown as ϵ_k. The overall efficiency $\epsilon_{\pi\pi J/\psi}$ for each of the three cases is also shown.

$N_{\rm trk}^{J/\psi}$	w_k (incl.)	w_k (BES)	w_k (CLEO-c)	ϵ_k(%)
0	0.0175	0.0225	0.0231	56.56
2	0.3440	0.3881	0.3945	55.82
4	0.4310	0.4015	0.4012	53.97
6	0.1871	0.1644	0.1627	52.03
8	0.0199	0.0200	0.0185	49.49
$\epsilon_{\pi\pi J/\psi}$ (%)	54.17	54.15	54.36	

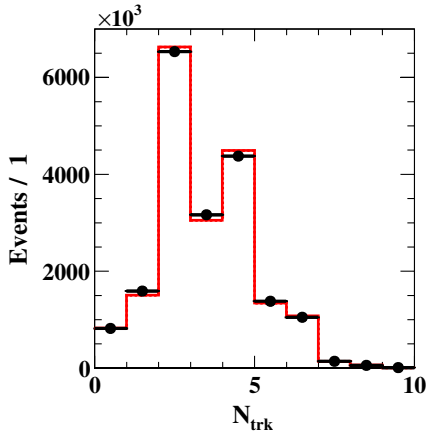

FIG. 5 (color online). Fit (histogram) to the multiplicity distribution of data (points) with that of the MC sample.

From the above analysis, the uncertainty from the charged track multiplicity distribution was found to be less than 0.2%, including all the contributions from the fit, the sideband selection, and the backgrounds. The efficiency does exhibit a weak dependence not only on the charged multiplicity, but also slightly on the neutral track multiplicity. More neutral particles in the J/ψ decay soften the momentum spectrum of the charged tracks, which makes the tracks harder to detect, and produces more photon conversions in the material in the inner detectors, which also changes the charged track multiplicity. But a MC study suggests that such effects are very small and can be neglected.

The dipion invariant mass distribution is simulated with the measurement of Ref. [22], in which a small amount of D-wave contribution is included. However, there is still a slight difference between the data and MC simulation, so the MC simulation is reweighted by the distribution in data, and the difference before and after the reweighting, which is 0.35% for $\epsilon_{\pi\pi J/\psi}$, is taken as a systematic uncertainty. The difference is much smaller for $\epsilon_{l^+l^-}$, $\sim$0.01%, since the effect cancels in a relative measurement.

The fit to the huge statistics of the distribution of mass recoiling against the dipion gave a poor χ^2/d.o.f., since the

resolutions in the exclusive and inclusive decays are a bit different. The signal shapes of the exclusive channel are smeared by convoluting with double Gaussian functions to improve the fit quality. As a result, $\mathcal{B}_{\pi\pi J/\psi}$ is changed by 0.37% before and after the smearing, which is taken as one of the systematic uncertainties.

The shapes of the invariant mass distributions of lepton pairs are affected by the simulation of final-state radiation (FSR), which is simulated with the PHOTOS package [27]. Differences between data and MC simulation are still observed. The invariant mass requirement on lepton pairs is studied by an alternative control sample, in which the lepton pairs are identified by the information of the EMC, MUC, and specific ionization (dE/dx) measured in the MDC, while demanding that $M^{\rm rec}_{\pi^+\pi^-}$ be consistent with the J/ψ mass, but without any requirement on the invariant mass of e^+e^- or $\mu^+\mu^-$. The differences are determined to be 0.29% (e^+e^-) and 0.45% ($\mu^+\mu^-$). To reduce this type of uncertainty, corrections are made based on this study, and the final contributions to the total systematic uncertainty are 0.10% and 0.23%, respectively.

The remaining sources of systematic uncertainty not addressed above are the requirements on E/p, the angles between the two leptons and the two pions, the background contamination for $\pi^+\pi^- l^+ l^-$ final states, and the uncertainty related to the fitting (counting) procedure. The first two items are determined with independent samples selected with alternative selection criteria, and the uncertainties of the E/p requirement are found to be 0.18% and 0.09% for muon and electron pairs, respectively; the uncertainties of the two angle requirements are found to be less than 0.1%. The uncertainties of the backgrounds of the $\pi^+\pi^- l^+ l^-$ exclusive final states are only $0.03 \sim 0.04\%$, after subtracting the background using known branching ratios. The uncertainties of the fitting (except the uncertainty of the resolution in $\mathcal{B}_{\pi\pi J/\psi}$), which are all at the part per thousand level, are estimated by changing the signal shape, background shape, fitting ranges (mass windows), and bin size. The uncertainties of the trigger efficiency in the three measurements are taken as 0.10% for $\mathcal{B}_{\pi\pi J/\psi}$ and 0.30% for $\mathcal{B}_{ll}$ according to the study in Ref. [28].

TABLE IV. Summary of the systematic uncertainties (%) in the branching fractions.

Sources	$\pi^+\pi^- J/\psi$	e^+e^-	$\mu^+\mu^-$
Tracking	0.80	0.20	0.20
Multiplicity of J/ψ	0.20	0.20	0.20
$M_{\pi^+\pi^-}$ distribution	0.35	0.01	0.01
Background shape	0.03	0.03	0.04
Fit/Count range	0.06	0.14	0.14
Bin size	0.06	0.06	0.06
E/p	···	0.18	0.09
$\cos\theta_{\pi^+\pi^-}$	0.13	0.07	0.07
$\cos\theta_{l^+l^-}$	···	0.04	0.05
FSR effect of l^+l^-	···	0.10	0.23
Fit method	0.37	0.37	0.37
Trigger	0.10	0.30	0.30
Number of $\psi(3686)$	0.81	···	···
Sum in quadrature	1.28	0.62	0.63

The systematic uncertainties in the branching fractions are summarized in Table IV. The systematic uncertainty in $\mathcal{B}[\psi(3686) \to \pi^+\pi^- J/\psi]$ is dominated by the number of $\psi(3686)$ events and the tracking efficiency of the two soft pions, and the total contribution of the other sources is less than 0.5%. The systematic uncertainty in $\mathcal{B}[J/\psi \to l^+l^-]$ is dominated by the uncertainty of the determination of $N_{\pi\pi J/\psi}$.

VII. SUMMARY AND DISCUSSION

The branching fractions of three processes $\psi(3686) \to \pi^+\pi^- J/\psi$, $J/\psi \to e^+e^-$, and $J/\psi \to \mu^+\mu^-$, were measured with $(106.41 \pm 0.86) \times 10^6$ $\psi(3686)$ decays. The results are $\mathcal{B}_{\pi\pi J/\psi} = (34.98 \pm 0.02 \pm 0.45)\%$, $\mathcal{B}_{ee} = (5.983 \pm 0.007 \pm 0.037)\%$, and $\mathcal{B}_{\mu\mu} = (5.973 \pm 0.007 \pm 0.038)\%$, where the first uncertainties are statistical and the second are systematic. We also measured $\mathcal{B}_{ee}/\mathcal{B}_{\mu\mu} = 1.0017 \pm 0.0017 \pm 0.0033$, where the common systematic uncertainties have been canceled out. This tests e-μ universality at the four tenths of a percent level. The precision is significantly improved with respect to the Particle Data Group average $\mathcal{B}_{ee}/\mathcal{B}_{\mu\mu} = 0.998 \pm 0.012$ [11]. Assuming leptonic universality, the average of $\mathcal{B}_{ee}$ and $\mathcal{B}_{\mu\mu}$ is $\mathcal{B}[J/\psi \to l^+l^-] = (5.978 \pm 0.005 \pm 0.040)\%$, in which the correlations among the uncertainties are accounted for. The measured branching fractions of $J/\psi \to e^+e^-/\mu^+\mu^-$ are consistent with previous measurements, and will allow for improvements in potential models [9] and the determinations of Γ_{ee} and $\Gamma_{\rm tot}$ of J/ψ [10].

Figure 6 shows a comparison of $\mathcal{B}_{\pi\pi J/\psi}$ among various experiments. Our measured $\mathcal{B}_{\pi\pi J/\psi}$ is the most precise to date and is consistent with the latest CLEO-c [5]

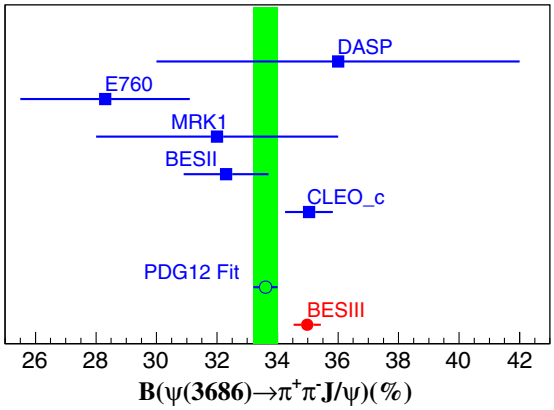

FIG. 6 (color online). Comparison of $\mathcal{B}[\psi(3686) \to \pi^+\pi^- J/\psi]$ among different experiments.

measurement, but higher than most of the previous measurements. This improved result of $B_{\pi\pi J/\psi}$, as well as the distribution of invariant mass of the two pions, can be used to determine parameters of some theoretical models [3,29]. Furthermore, a higher precision of this measurement would be a good test for the next-to-leading-order effects such as relativistic correction [30].

ACKNOWLEDGMENTS

The BESIII collaboration thanks the staff of BEPCII and the computing center for their strong support. This work is supported in part by the Ministry of Science and Technology of China under Contract No. 2009CB825200; the National Natural Science Foundation of China (NSFC) under Contracts No. 10625524, No. 10821063, No. 10825524, No. 10835001, No. 10935007, No. 11125525, No. 11235011, and No. 11005115; the Joint Funds of the National Natural Science Foundation of China under Contracts No. 11079008, No. 11179007, and No. 10979058; the Chinese Academy of Sciences (CAS) Large-Scale Scientific Facility Program; CAS under Contracts No. KJCX2-YW-N29 and No. KJCX2-YW-N45; the 100 Talents Program of CAS; the German Research Foundation DFG under Contract No. Collaborative Research Center CRC-1044; the Istituto Nazionale di Fisica Nucleare, Italy; the Ministry of Development of Turkey under Contract No. DPT2006K-120470; the U.S. Department of Energy under Contracts No. DE-FG02-04ER41291, No. DE-FG02-05ER41374, and No. DE-FG02-94ER40823; the U.S. National Science Foundation; University of Groningen (RuG) and the Helmholtzzentrum fuer Schwerionenforschung GmbH (GSI), Darmstadt; and the WCU Program of National Research Foundation of Korea under Contract No. R32-2008-000-10155-0.

[1] J. J. Aubert *et al.* (E598 Collaboration), Phys. Rev. Lett. **33**, 1404 (1974); J. E. Augustin *et al.*, Phys. Rev. Lett. **33**, 1406 (1974).
[2] K. Gottfried, Phys. Rev. Lett. **40**, 598 (1978).
[3] L. S. Brown and R. N. Cahn, Phys. Rev. Lett. **35**, 1 (1975).
[4] G. S. Abrams *et al.*, Phys. Rev. Lett. **34**, 1181 (1975).
[5] H. Mendez *et al.* (CLEO Collaboration), Phys. Rev. D **78**, 011102(R) (2008).
[6] B. H. Wiik, http://epub.sub.uni-hamburg.de/epub/volltexte/2011/9663/pdf/DESY_75_37.
[7] T. A. Armstrong *et al.* (E760 Collaboration), Phys. Rev. D **55**, 1153 (1997).
[8] J. Z. Bai *et al.* (BES Collaboration), Phys. Lett. B **550**, 24 (2002).
[9] C. Quigg and J. L. Rosner, Phys. Rep. **56**, 167 (1979); A. K. Grant, J. L. Rosner, and E. Rynes, Phys. Rev. D **47**, 1981 (1993); D. Besson and T. Skwarnicki, Annu. Rev. Nucl. Part. Sci. **43**, 333 (1993); N. Brambilla *et al.* (Quarkonium Working Group), arXiv:hep-ph/0412158.
[10] B. Aubert *et al.* (*BABAR* Collaboration), Phys. Rev. D **69**, 011103 (2004).
[11] J. Beringer *et al.* (Particle Data Group), Phys. Rev. D **86**, 010001 (2012).
[12] Z. Li *et al.* (CLEO Collaboration), Phys. Rev. D **71**, 111103(R) (2005).
[13] J. Z. Bai *et al.* (BES Collaboration), Phys. Rev. D **58**, 092006 (1998).
[14] M. Ablikim *et al.* (BESIII Collaboration), Nucl. Instrum. Methods Phys. Res., Sect. A **614**, 345 (2010).
[15] J. Z. Bai *et al.* (BES Collaboration), Nucl. Instrum. Methods Phys. Res., Sect. A **458**, 627 (2001).
[16] D. M. Asner *et al.*, Int. J. Mod. Phys. A **24**, 499 (2009); arXiv:0809.1869.
[17] M. Ablikim *et al.* (BESIII Collaboration), Chinese Phys. C **37**, 063001 (2013); arXiv:1209.6199.
[18] S. Jadach, B. F. L. Ward, and Z. Was, Phys. Rev. D **63**, 113009 (2001).
[19] R.-G. Ping, Chinese Phys. C **32**, 599 (2008).
[20] W.-M. Yao *et al.* (Particle Data Group), J. Phys. G **33**, 1 (2006).
[21] J. C. Chen, G. S. Huang, X. R. Qi, D. H. Zhang, and Y. S. Zhu, Phys. Rev. D **62**, 034003 (2000).
[22] J. Z. Bai *et al.* (BES Collaboration), Phys. Rev. D **62**, 032002 (2000).
[23] E. Barberio and Z. Was, Comput. Phys. Commun. **79**, 291 (1994).
[24] S. Agostinelli *et al.* (GEANT4 Collaboration), Nucl. Instrum. Methods Phys. Res., Sect. A **506**, 250 (2003); J. Allison *et al.*, IEEE Trans. Nucl. Sci. **53**, 270 (2006).
[25] Y. Kubota *et al.* (CLEO Collaboration), Nucl. Instrum. Methods Phys. Res., Sect. A **320**, 66 (1992); D. Peterson *et al.*, Nucl. Instrum. Methods Phys. Res., Sect. A **478**, 142 (2002); M. Artuso *et al.*, Nucl. Instrum. Methods Phys. Res., Sect. A **502**, 91 (2003).
[26] J. Z. Bai *et al.* (BES Collaboration), Nucl. Instrum. Methods Phys. Res., Sect. A **344**, 319 (1994).
[27] E. Barberio and Z.Was, Comput. Phys. Commun. **79**, 291 (1994).
[28] N. Berger, Z.-A. Liu, D.-P. Jin, H. Xu, W.-X. Gong, K. Wang, and G.-F. Cao, Chinese Phys. C **34**, 1779 (2010).
[29] H. Y. Zhou and Y. P. Kuang, Phys. Rev. D **44**, 756 (1991); Y. P. Kuang and T. M. Yan, Phys. Rev. D **41**, 155 (1990); M. Chemtob and H. Navelet, Phys. Rev. D **41**, 2187 (1990); T. Mannel and R. Urech, Z. Phys. C **73**, 541 (1997).
[30] M. B. Voloshin, Phys. Rev. D **74**, 054022 (2006).